Comparison and analysis of two aerosol retrievals over the ocean in the Terra/Clouds and the Earth's Radiant Energy System–Moderate Resolution Imaging Spectroradiometer single scanner footprint data: 2. Regional evaluation

Tom X.-P. Zhao,[1,2] Istvan Laszlo,[2] Patrick Minnis,[3] and Lorraine Remer[4]

[1] The advanced multichannel Moderate Resolution Imaging Spectroradiometer (MODIS) and simple independent two-channel Advanced Very High Resolution Radiometer (AVHRR) aerosol retrieval algorithms were compared regionally using the Terra/CERES-MODIS Single Scanner Footprint (SSF) data. On average, it was found that the two methods tend to overestimate 0.66-μm aerosol optical thickness (AOT) compared to AERONET surface observations in the original SSF data. If the most cloud-free data are used, the mean satellite retrievals agree to within ±10% of the AERONET data. The MODIS near-infrared (1.60-μm) AOTs are in better agreement with the surface data than the AVHRR-type retrievals. The satellite-derived aerosol size parameters are 20–30% smaller than the surface-based values with the MODIS values closer to the AERONET values than that of AVHRR-type. The effects of aerosol model assumptions, cloud contamination, and surface roughness on the two aerosol retrievals were analyzed in detail with the careful classification of clear-sky and surface roughness conditions. For most of the regions examined, the annual mean AOTs from the MODIS retrieval are 0.03 and 0.02 less than their AVHRR-type counterparts at 0.66 and 1.60 μm, respectively. However, the MODIS values may exceed the AVHRR-type values in regions where the prevailing aerosol type varies with season or is under an apparent influence of cloud or surface disturbance. Examination of the surface treatments used by the two retrieval methods indicates the need for improvement over very rough ocean surfaces, especially for the AVHRR method. The results indicate that aerosol model assumptions become important for regional retrievals and the dynamic aerosol models used in the MODIS retrieval are better suited for simultaneously measuring the regional variations in aerosol optical properties and their global mean values.

1. Introduction

[2] The distribution and composition of tropospheric aerosols vary substantially both spatially and temporally because of their various emission sources, sinks and short lifetimes. These variations cause the largest uncertainties in assessing the radiative forcing of climate by atmospheric constituents generated by anthropogenic activities [*Intergovernmental Panel on Climate Change*, 2001]. Because of daily global coverage, satellite observations have been widely used for monitoring the distribution of aerosol particles [*King et al.*, 1999; *Kaufman et al.*, 2002; *Mishchenko et al.*, 2004]. However, satellite aerosol retrievals require a very careful separation of the relatively weak aerosol signal from the other factors influencing the retrieval including those associated with radiometric and calibration errors of the sensor, inaccurate assumptions in the retrieval algorithm, variable atmospheric gas absorption and surface reflectance, and cloud contamination [*Tanré et al.*, 1996; *Mischenko et al.*, 1999]. The regional impact of these uncertainties on the final satellite aerosol products are expected to be larger than their impact on the global scale. Thus the uncertainties in satellite aerosol retrievals should be evaluated on both global and regional scales.

[3] *Zhao et al.* [2005], in the first part of this two-part paper, performed a global comparison and evaluation of the

[1]Earth System Science Interdisciplinary Center, University of Maryland, College Park, Maryland, USA.
[2]Office of Research and Application, NOAA National Environmental Satellite, Data, and Information Service, Camp Springs, Maryland, USA.
[3]Atmospheric Sciences Division, NASA Langley Research Center, Hampton, Virginia, USA.
[4]Laboratory for Atmospheres, NASA Goddard Space Flight Center, Greenbelt, Maryland, USA.

Table 1. Nineteen Locations Selected for the Regional Comparison of the Two SSF Aerosol Products[a]

	Location (Abbreviation)[b]	Latitude, Longitude	Major Aerosol Type[c]
1	Andros Island (AND)	24.68°, −77.78°	U/I, M
2	Ascension Island (ASC)	−7.97°, −14.40°	B, D, M
3	Bahrain (BAH)	26.32°, 50.50°	D, U/I
4	Barbados (BAR)	13.17°, −59.50°	D, M, U/I
5	Bermuda (BER)	32.37°, −64.68°	U/I, M
6	Cape Verde (CAP)	16.72°, −22.93°	D
7	Dakar (DAK)	14.38°, −16.95°	D, B
8	Dry Tortugas (DRY)	24.60°, −82.78°	U/I, M, D
9	Guadeloup (GUA)	16.32°, −61.50°	U/I, M, D, B
10	Kaashidhoo (KAA)	4.95°, 73.45°	M, D
11	Lanai (LAN)	20.82°, 156.98°	M
12	San Nicolas (SAN)	33.25°, −119.49°	M, U/I
13	Surinam (SUR)	−5.78°, −55.20°	D, B
14	North Pacific Ocean (NPC)	20.00°, −130.00°	M
15	South Pacific Ocean (SPC)	−45.00°, −120.00°	M
16	North Atlantic Ocean (NAT)	20.00°, −30.00°	D, M
17	South Atlantic Ocean (SAT)	−30.00°, −20.00°	M, B
18	South Indian Ocean (SIN)	−45.00°, 80.00°	M
19	East Coast of China (ECC)	30.00°, 150.00°	M, U/I, D

[a]Their geographical location (latitude, longitude) and the major aerosol types observed over them are indicated.
[b]The first 13 locations are AERONET sites.
[c]B, D, M, U/I represent biomass-burning aerosol, dust aerosol, marine aerosol, and urban/industrial aerosol, respectively.

aerosol properties derived from one year of Terra Moderate Resolution Imaging Spectroradiometer (MODIS) measurements using two retrieval methods, the multichannel MODIS science team technique and the independent two-channel NOAA/NESDIS Advanced Very High Resolution Radiometer (AVHRR) method (hereafter referred to as the MODIS and AVHRR-type methods). It was found that, in a global mean average, the aerosol optical thickness values were comparable for the two methods although the AVHRR-type values tended to be slightly larger overall in very clear conditions. Cloud and surface roughness appear to affect both aerosol retrievals. The global comparison and analysis [*Zhao et al.*, 2005] can be considered as the first-order evaluation. Detailed regional comparison and analysis are also needed for a more complete (or second-order) evaluation of the two SSF aerosol retrievals. In this second paper, results from the two methods are evaluated at the regional scale using the same Terra Clouds and the Earth's Radiant Energy System (CERES) Single Scanner Footprint (SSF) data introduced in section 2 of the first paper. Cloud and surface roughness effects on the two retrievals are also further examined.

2. Regional Comparison and Validation

[4] The SSF data used here are described in detail by *Zhao et al.* [2005]. The aerosol properties were derived using the two methods applied to the same MODIS data. In addition to differences in the retrieval methodologies, the specific pixels used in the retrievals can differ because of differences in the cloud screening methods associated with each technique. Hereafter, the AVHRR-type retrieval is referred to as the AVHRR retrieval with the understanding that it refers to MODIS data analyzed with the AVHRR-type retrieval method.

2.1. Statistical Comparison

[5] The regional comparison presented in this section will focus on the study of the original SSF aerosol data defined in the first paper. Here, nineteen locations (listed

in Table 1) over the globe were selected for this purpose. The first thirteen locations are Aerosol Robotic Network (AERONET) sites [*Holben et al.*, 1998, 2001], which were carefully selected to represent the marine environment and cover the four major aerosol types (biomass burning, mineral dust, maritime, and urban industrial) over the global oceans. The AERONET observations at these sites are used here as independent measurement or "ground truth" for the evaluation of the two SSF satellite aerosol products. The last six locations in Table 1 were selected because they are located in remote ocean areas and in the regions where the two SSF aerosol products show relatively large differences in the previous comparison of the aerosol global distributions. The prevailing aerosol types over the 19 locations are also indicated in Table 1. For each site, the intercomparison of the two satellite aerosol products was performed for the SSF footprints contained in a 5° × 5° box over the site to include sufficient footprints for statistics.

[6] Figure 1 displays the differences (AVHRR − MODIS) in the mean values of aerosol optical thickness, $\Delta\tau_i$, at the 19 sites for January, April, July, and October of 2001. The subscript, $i = 1$ and 2, refers to the wavelengths 0.66 μm and 1.60 μm, respectively. For the 4-month average (the solid lines in Figure 1), the AVHRR values are generally larger than the MODIS values in both channels ($\Delta\tau_1 < 0.03$ and $\Delta\tau_2 < 0.02$) at most sites. Only at the three ocean sites (SAT, SIN, and SPC) in the Southern Hemisphere middle latitudes, the AVHRR values fall below their MODIS counterparts. During January and October, $\Delta\tau_1$ and $\Delta\tau_2$ at the SAN and ECC sites dip to values close to or less than zero. The specific features observed in Figure 1, especially those at BAH, CAP, ECC, NPC, SAN, SAT, SIN, and SPC, deserve further investigation.

[7] Scatter diagrams of the channel 1 aerosol optical thickness (AOT) for January, April, July, and October are plotted in Figures 2 and 3 for 7 selected sites: ECC, SAN, SAT, SPC, BAH, CAP, and NPC. These sites were chosen because $\Delta\tau_1$ is relatively large or $\Delta\tau_1$ shows strong seasonal variations in Figure 1. The linear fits, correlation coefficients (r), and root-mean-square (RMS) differences are also
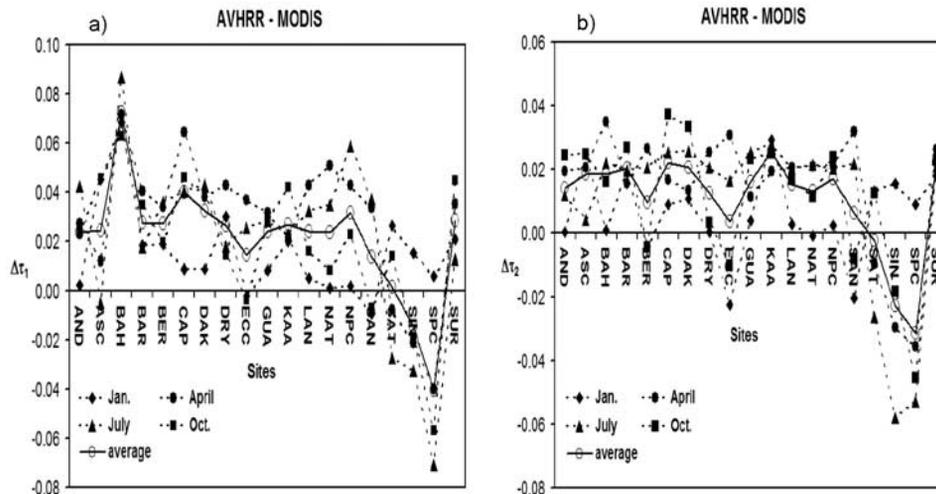
Figure 1. Mean difference (AVHRR-MODIS) in AOT at 19 selected locations for January, April, July, and October 2001 and the 4-month averages, (a) channel 1 ($\lambda_1 = 0.66$ μm) and (b) channel 2 ($\lambda_2 = 1.64$ μm). Lines connecting the symbols are for illustration purposes only.

shown in each plot. The MODIS and AVHRR τ_1 values agree reasonably well at ECC especially during January and October with relatively little scatter compared to April and July when the τ_1(MODIS) is slightly less than τ_1(AVHRR). The differences in the two AOTs at SAN are somewhat larger than those at ECC with more outliers and lower correlations during January. At SAT, the τ_1(MODIS) and τ_1(AVHRR) agree well, on average, during April and October but the RMS differences during January, July, and October are more double those during April. At SPC, the outliers with τ_1(MODIS) $\gg \tau_1$(AVHRR) in the scatterplot have a significant impact on the average differences, a subject of further investigation later in this paper. At BAH and CAP in Figure 3, τ_1(AVHRR) is systematically greater than τ_1(MODIS), especially during January and April at BAH and during April, July, and October at CAP. The RMS differences at BAH are relatively large for all months but vary seasonally at CAP. At NPC, the differences in the AOTs are most striking during April and July. The scatter is least during January and greatest during the spring and summer.

[8] The probability distribution functions (PDF) of τ_1 at BAH, ECC, NPC, and SPC, plotted in Figure 4 for the 4 months, are used to further examine the statistical differences between the two SSF aerosol data sets. At Bahrain (BAH), the AVHRR distribution (dashed line) is skewed toward high values in all 4 months, while τ_1(MODIS) peaks around $\tau_1 = 0.3$ for all months but July. However, the two distributions agree reasonably well off the east coast of China (ECC), especially during January and October. At NPC, the PDFs are nearly identical in January, while τ_1(AVHRR) spreads slightly more than τ_1(MODIS) during April, July, and October. At the remote South Pacific site (SPC), the MODIS and AVHRR PDFs agree reasonably well in January, April, and October. A significant difference is observed during July.

[9] As an initial comparison with the surface observations, the PDFs of τ_1 at the AERONET sites, BER, CAP, DRY, and LAN (the only four AERONET sites with surface observations in all 4 months) are plotted in Figure 5 with the two SSF PDFs. The AERONET data can be considered as a "calibration reference" since they are from highly accurate measurements. At BER, the PDFs of the three observations agree reasonably well in January and July. All three PDFs show double peaks in July, although the peak locations differ slightly and the AVHRR secondary peak is less pronounced. In April and October, the MODIS and AVHRR PDFs are relatively broad, while the AERONET distribution is confined within a narrow range with modal values τ_1(m) of ~0.23 and 0.10 in April and October, respectively. At the dusty Cape Verde site (CAP), the three PDFs are most similar during January. They depart from each other in the other 3 months with the satellite-based distributions skewed toward low values in July and October. At DRY, the three distributions agree reasonably well in July and October. The two satellite PDF distributions are similar in January and April while the AERONET PDF tends to have a narrower spread and is skewed toward low AOT in April. In January, the AERONET PDF is distorted because of poor sampling (only 15 measurements are available for the PDF statistics). Over the typical marine site LAN, the three PDFs have similar modal values in all 4 months. The two satellite distributions agree better in shape but are wider than the AERONET PDF.

2.2. Ensemble AERONET Validation

[10] To further assess the accuracy of the mean MODIS and AVHRR-type aerosol products, they are compared directly with the surface-based measurements of τ_1, τ_2, and α (Ångström exponent) at all thirteen AERONET sites listed in Table 1. These locations were selected as the baseline validation sites for the operational AVHRR aerosol retrieval [Zhao et al., 2002] and cover the four major aerosol types (urban/industrial, biomass burning, maritime, and dust) over the global oceans. The selection criteria for these sites were discussed by Zhao et al. [2002, 2003]. Quality assured Level 2 AERONET data [Smirnov et al., 2000] are used here as the "ground truth"
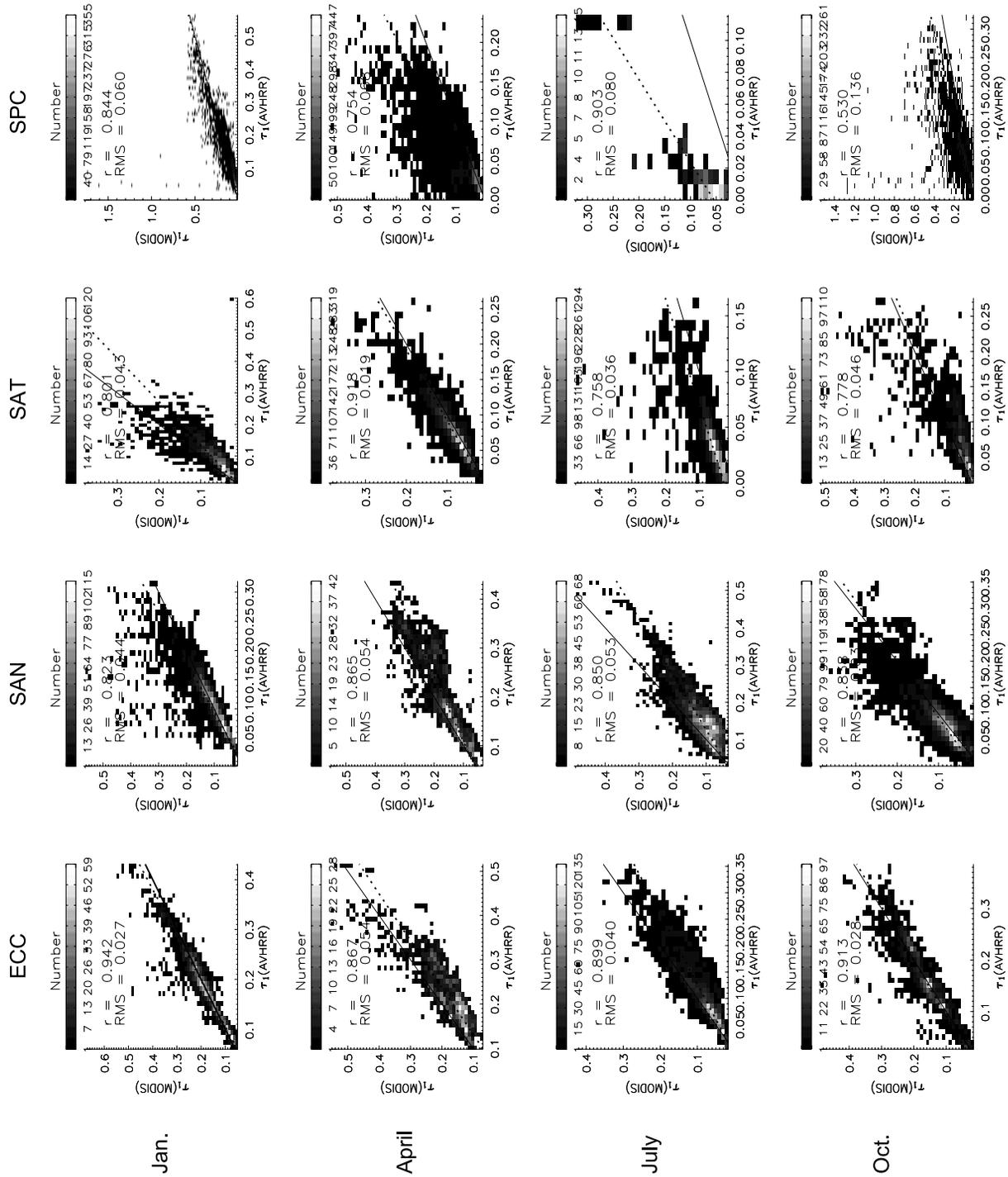
Figure 2. Scatterplots of τ_l(MODIS) versus τ_l(AVHRR) over ECC, SAN, SAT, and SPC sites during 2001. Number density of the points is represented by the brightness. Solid line is 1:1 relationship. Dashed line is linear fit.
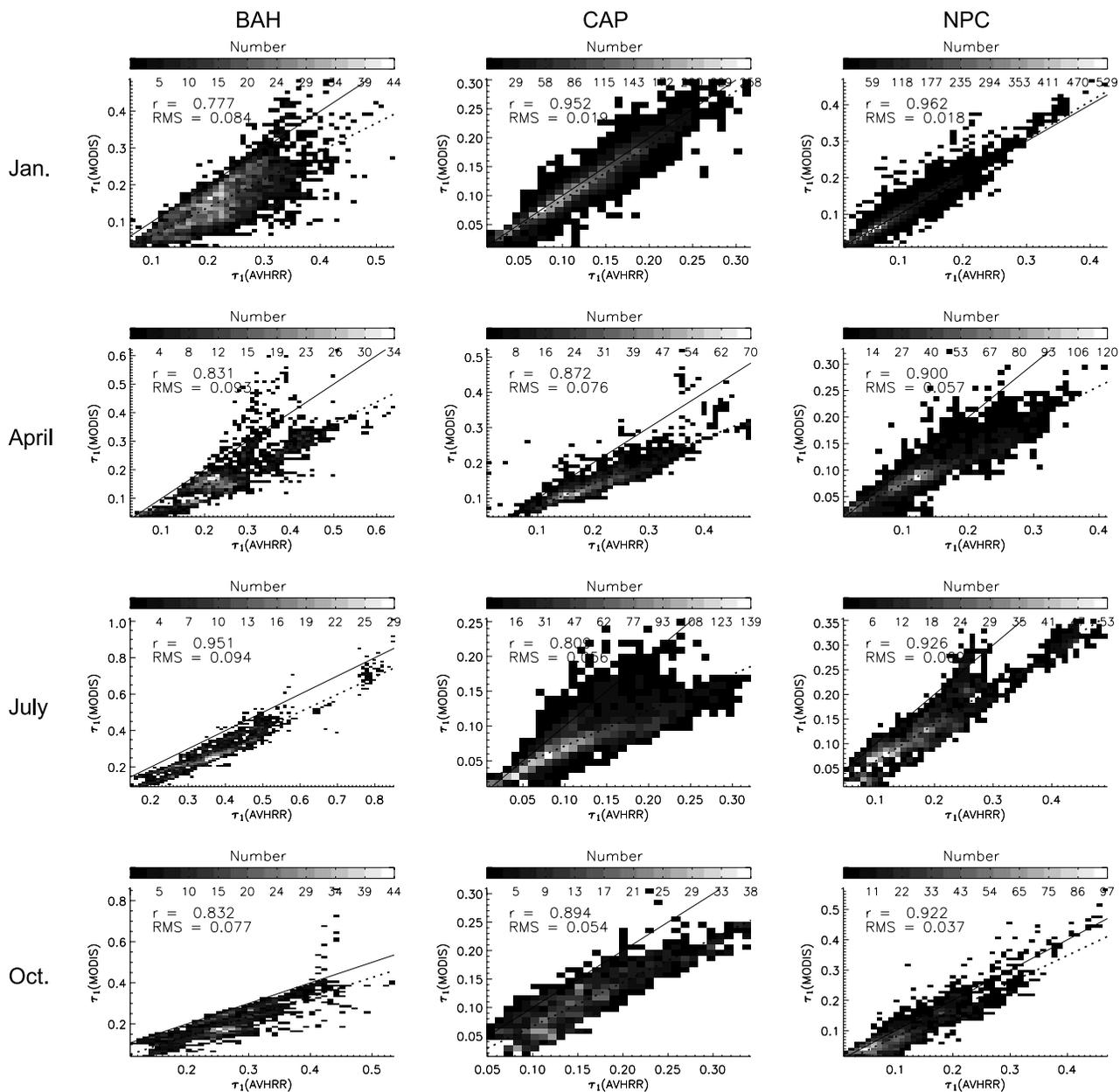
Figure 3. Same as Figure 2 except for BAH, CAP, and NPC sites.

set. The spatial match-up window consists of an outer circle with a 150-km radial distance from the site, excluding an inner circle (with a fixed radius of 25 km) to reduce the effects of coastline or shallow water influences. The temporal match-up window is ±1 hour within the satellite overpass time. Thus each overpass (or match-up point) contains multiple AERONET and satellite pixels. Their averaged values are used as overpass (or match-up) values for the AERONET and the two satellite retrieval results.

[11] The match-up points found during 2001 over the 13 sites are combined to make an ensemble validation. A total of 110 match ups were found; most are from three sites, Bermuda, Dry Tortugas, and Lanai so that the dynamic range in τ is small and the scatterplot comparisons are relatively meaningless. Only the ensemble mean comparison makes sense and, therefore, is presented here

for two scenarios. The first is for the original match-up points. The second is for the strong clear situation determined by selecting the match-up records using SSF pixels having a clear strong index (CSI, see *Zhao et al.* [2005]) > 90% from the original overpass records at the match-up points. The resampled records for each overpass are then averaged to obtain the new values for the match-up point. The final matched points are reduced to 79 in the strong clear scenario because of the resampling.

[12] The results of the ensemble validation for the two scenarios are summarized in Figure 6 for three aerosol variables τ_1, τ_2 and α. For the original match ups, there are obvious differences in the each variable for the three retrieval methods. In all cases, $\tau(AVHRR)$ is greater than τ from the other methods and $\tau(MODIS)$ exceeds $\tau(AERONET)$ when no strong clear conditions are applied. Conversely, $\alpha(AERONET)$ exceeds both satellite

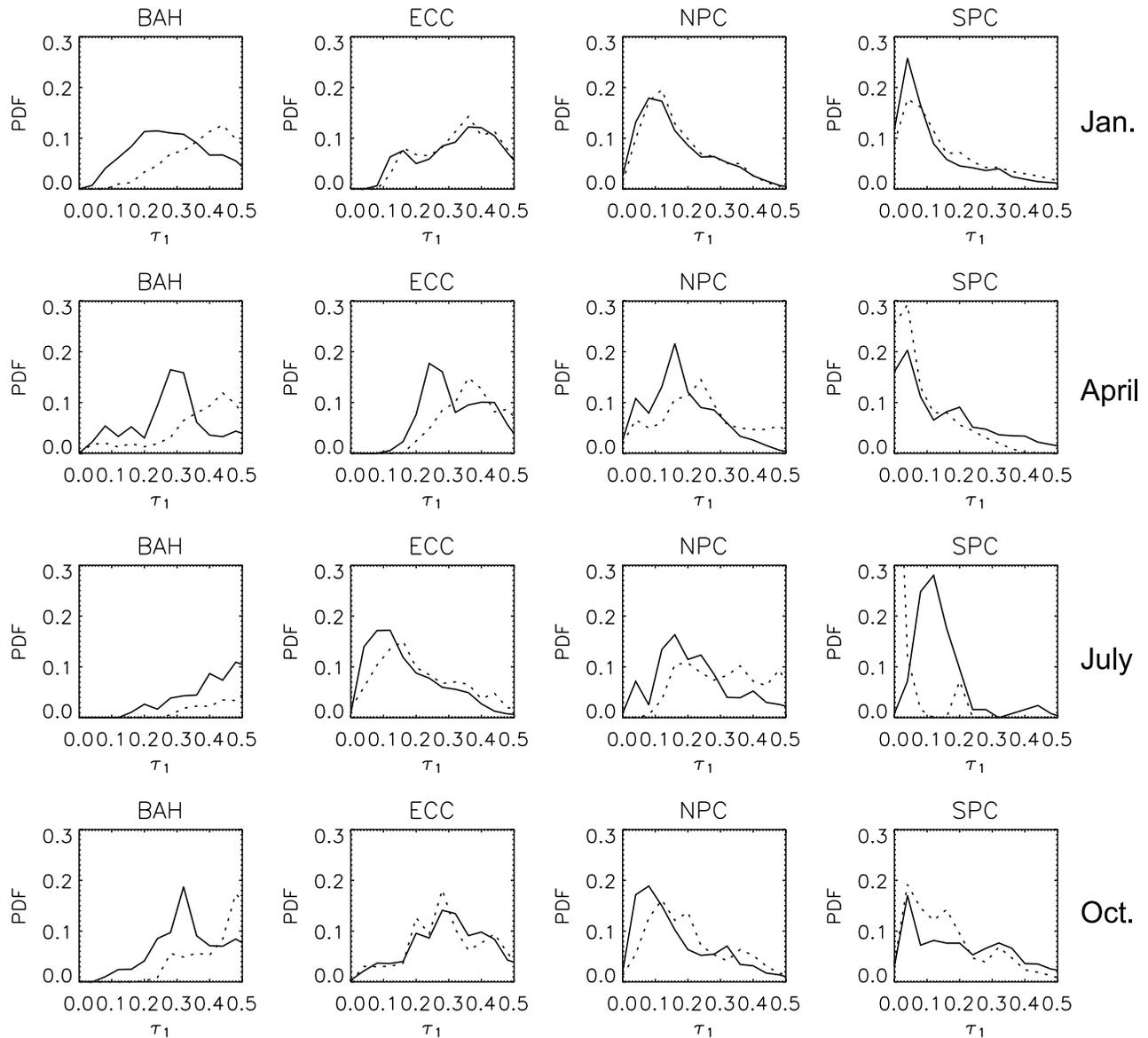**Figure 4.** Probability distribution functions of τ_1(MODIS) (bold) and τ_1(AVHRR) (dashed) observed during 2001 over selected sites.

retrievals regardless of conditions. For the strong clear scenario, the MODIS and AVHRR AOTs are in much better agreement with the AERONET values than in the original match ups. The absolute differences among τ_1(AERONET), τ_1(MODIS), and τ_1(AVHRR) are nearly identical for the strong clear conditions, while τ_2(MODIS) is closer than τ_2(AVHRR) to τ_2(AERONET). These results confirm that both the MODIS and AVHRR retrievals are subject to some cloud effects. Considering that quality controlled AERONET data are collected in relatively clear conditions and compare better with the two satellite data sets in the strong clear scenario, it is reasonable to conclude that the cloud effects on the original match-up data of the two SSF aerosol products are mainly due to residual subpixel cloud contamination rather than to real aerosol signals in the vicinity of clouds. This conclusion is also supported by the fact that the AERONET τ is the same for the two scenarios, but both satellite values drop

in cloud-free conditions. If the aerosol were really different in the two situations, then the AERONET value would drop also. The impact of the cloud effects will be further explored in section 3.

[13] After cloud contamination has been reduced by selecting strong clear match ups, the remaining differences between the AVHRR and MODIS values are due to differences in the two retrieval algorithms (such as the aerosol model assumptions or surface treatment), which are investigated later. Figure 6 demonstrates that the ensemble mean of AOT derived from the simple independent two-channel AVHRR retrieval is comparable to that derived from the multichannel MODIS aerosol retrieval (e.g., $\Delta\tau_1 \sim 0.02$ & $\Delta\tau_2 < 0.02$) for the sample of stations that are dominated by clean, background marine aerosols. This is not unexpected since the AVHRR-type retrieval was designed with an average marine aerosol model. However, aerosols originating over land because of human activities (such as smoke,
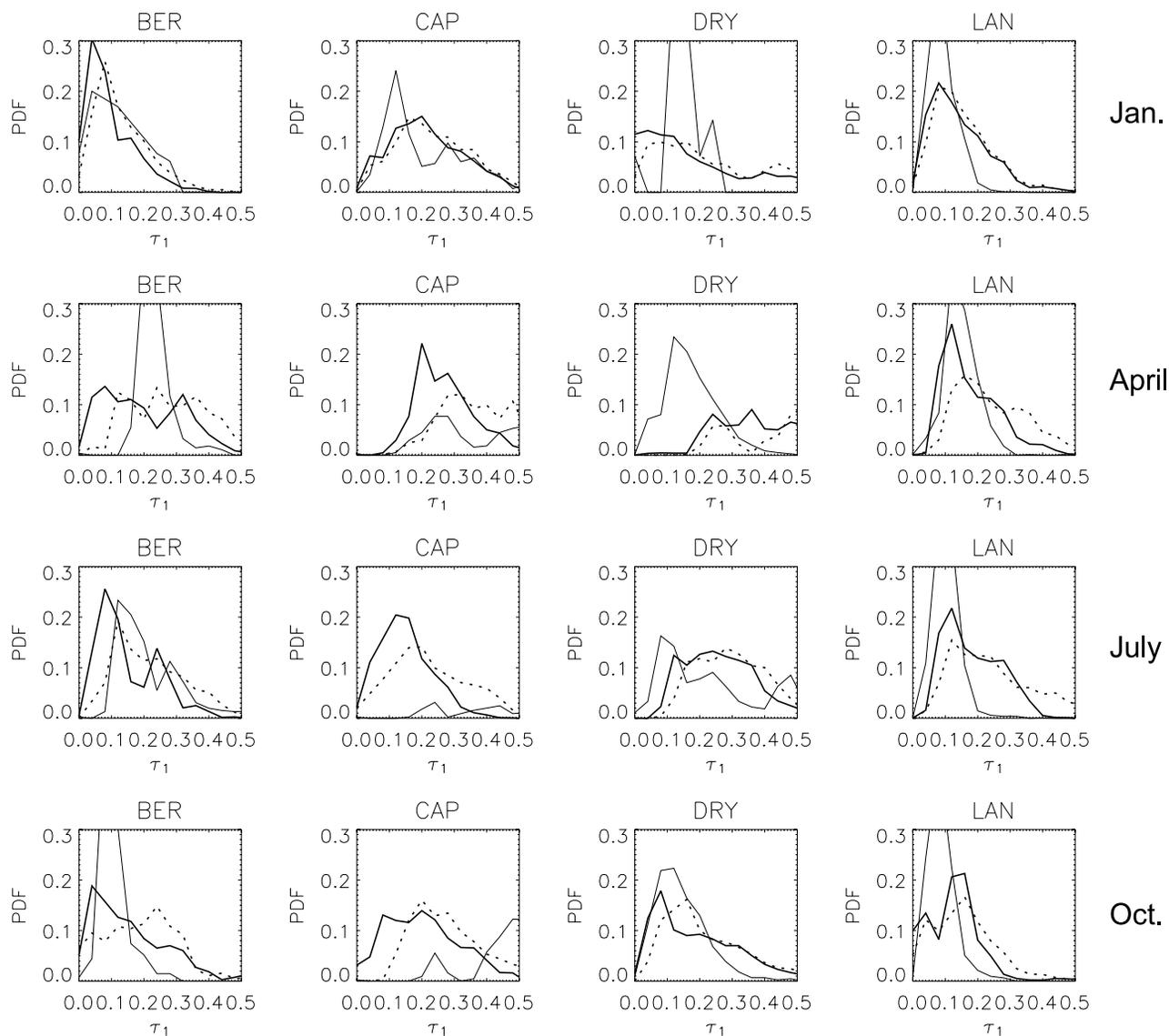
Figure 5. Same as Figure 4 except for BER, CAP, DRY, and LAN sites. AERONET observation is added (thin line).

dust, and industrial pollution) and natural events (e.g., sand storms and forest fires) are often transported over the global oceans. For example, carbonaceous aerosols from either biomass burning or pollution are advected from parts of Africa, South and Central America, India and South East Asia over the adjacent oceans during the dry seasons. Desert dust travels eastward across the Atlantic and westward over the Pacific Oceans following well-defined seasonal cycles. Since the properties of these aerosol types differ significantly from each other and from marine aerosols, the multispectral retrieval should be important for improving the aerosol optical thickness retrievals in situations when the aerosol over ocean is dominated by advected smoke, pollution, or dust, which will be demonstrated below in the analysis of section 3.

[14] The difference between α(AERONET) and α(MODIS) in Figure 6 for the strong clear scenario is almost the same as for the original match ups, but the corresponding difference between the AERONET and AVHRR-type retrievals increases in the strong clear sce-

nario. A similar increase in the difference between α(MODIS) and α(AVHRR) occurs for the strong clear conditions. This enhanced difference is likely due to the differences, such as the aerosol model assumption, in the two algorithms. The ensemble comparison to the AERONET ground truth suggests that cloud contamination masks the fundamental differences in the aerosol optical properties between the AVHRR aerosol model and the actual values. Thus the improvement in the aerosol retrievals from the multichannel algorithm relative to the simple two-channel algorithm in clean background marine aerosol condition is mainly seen in the size parameters rather than in optical thickness.

3. Analysis and Discussion

[15] Further analyses were performed to identify the causes of the differences observed in the above regional comparisons. Cloud effects, surface roughness, and aerosol model assumptions in the retrieval algorithms, the
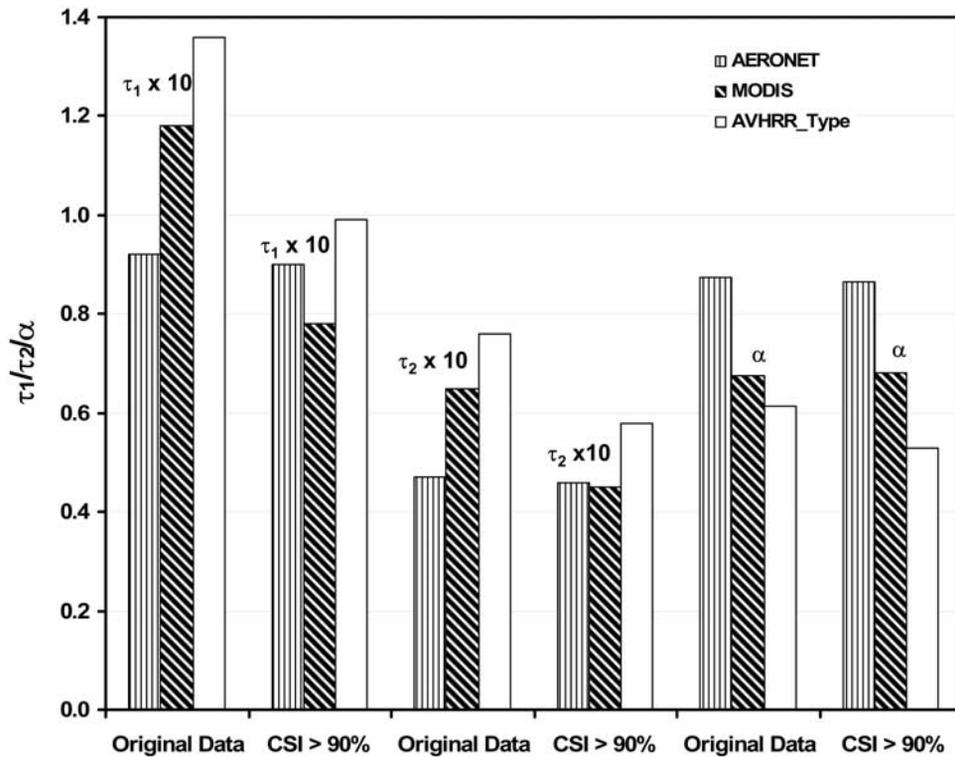
Figure 6. Comparison of τ_1 and τ_2, and α for matched SSF and AERONET observations at all 13 AERONET sites.

three major potential contributors to the differences in the two SSF aerosol products suggested in the global analysis [*Zhao et al.*, 2005], are still the focus of current studies.

[16] *Zhao et al.* [2005] found that subpixel cloud contamination is present in the two SSF aerosol products. However, not all cloud effects observed in the global comparison are necessarily the result of contamination. Actually, aerosol optical thickness can increase in proximity to clouds. Because of the high spatial resolution of the MODIS measurements, aerosol retrievals can be performed closer to clouds and the enhanced aerosols near the clouds may be detected. In addition, surface roughness may not only affect the aerosol retrievals but also may be physically linked to an enhancement of aerosols over a rough ocean surface due to injections from bubble bursts and the evaporation of sea spray. Therefore it is worthwhile to give a further correlation analysis on these effects on a regional scale since the problem can be more easily defined regionally compared to globally.

[17] The following regional analysis focuses on the same sites used in the above comparison. As in the global comparison, three CERES SSF-based parameters, CSI, Cloud Fraction (CF), and Surface Wind Speed (SWS), are used to define the extent of clear-sky and cloudy conditions and surface roughness for each CERES footprint. Four sets of conditions were analyzed for January, April, July, and October: (1) the original data with no restrictions; (2) the strong clear condition, CSI > 90%; (3) the smoothest surface condition, SWS < 3 m/s; and (4) the clearest and smoothest condition, the combination of cases 2 and 3. In contrast to the global comparison, a larger wind speed was

selected to ensure a sufficient number of retrievals are used in the analysis.

[18] The eight sites, BAH, CAP, ECC, NPC, SAN, SAT, SIN, and SPC, selected from Figure 1, were further divided into three groups. The first group includes BAH, CAP, and NPC where τ_1(MODIS) is systematically lower than τ_1(AVHRR). The second group consists of ECC and SAN where $\Delta\tau$ varies seasonally. Last, the third group includes SAT, SIN and SPC where τ_1(MODIS) is systematically greater than τ_1(AVHRR) during most of the year.

3.1. Group One Analysis

[19] In analyzing the first group, τ_1(MODIS) is compared with τ_1(AVHRR) in scatterplots for case 4 separately for each month. In Figure 7, τ_1(AVHRR) is systematically higher than τ_1(MODIS) during all 4 months over the BAH site. It is known that errors introduced by incorrect surface assumptions mainly affect the offset of a linear regression (e.g., solid lines in Figure 7) between the two aerosol retrievals while the errors introduced by incorrect aerosol model assumptions mainly affect the slope [*Zhao et al.*, 2002, 2003]. Since the effects of clouds and surface roughness have been minimized in the clearest and smoothest case, the remaining differences in the two AOTs are expected to be due to differences in the aerosol model assumptions and/or the treatment of surface reflectance. Considering that very similar features are also observed in the case of the original data (Figure 3), it is reasonable to conclude that these same factors caused the large differences in the BAH MODIS and AVHRR retrievals. A similar conclusion was also obtained for the CAP site.
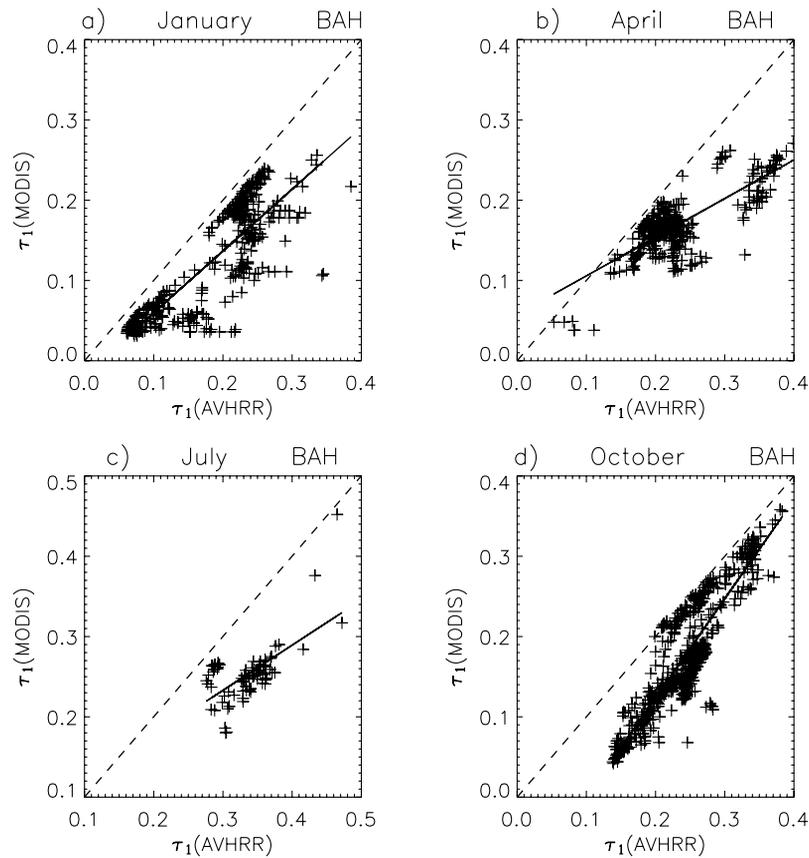
Figure 7. Scatterplots of τ_1(MODIS) versus τ_1(AVHRR) for CSI > 90% and SWS < 3 m/s at the BAH site. Dashed line is the 1:1 relationship, and solid line is the linear fit.

[20] Both BAH and CAP are dust sites with relatively large AOTs. Slightly enhanced aerosol absorption is expected at BAH because of mixing with industrial particles [*Dubovik et al.*, 2002]. The aerosol model assumptions in a retrieval algorithm are important for an accurate derivation of the AOT over these two sites. Larger errors are expected for the AVHRR-type retrieval at these two sites since a globally fixed aerosol model is used in the retrieval algorithm [*Zhao et al.*, 2004]. Even for the MODIS retrieval, which is based on a dynamic aerosol model, the derived AOT disagrees as much with the AERONET observations

(Figure 5 for the CAP site) as the AVHRR-type retrieval. This may be due to the fact that, unlike the AERONET retrieval, the nonspherical effect of dust particles is included in neither the MODIS nor the AVHRR-type retrievals.

[21] The NPC is over a remote part of the north Pacific where maritime aerosols predominate except in spring and summer when Asian dust and pollution intrusions are common. For the clearest and smoothest case, it is anticipated that the MODIS and AVHRR-type retrievals should be close to each other for this marine site in the winter months, but not in the spring and summer months
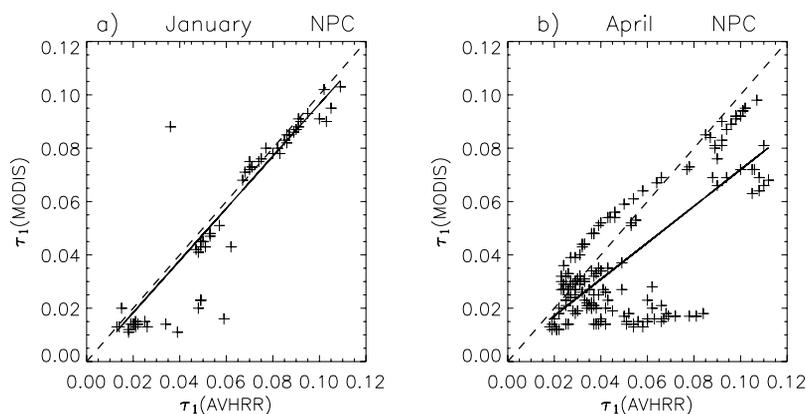

Figure 8. Same as Figure 7 except for NPC. No footprints satisfy the conditions, CSI > 90% and SWS < 3 m/s, in July and October.

Figure 9. Same as Figure 7 except for SAN.
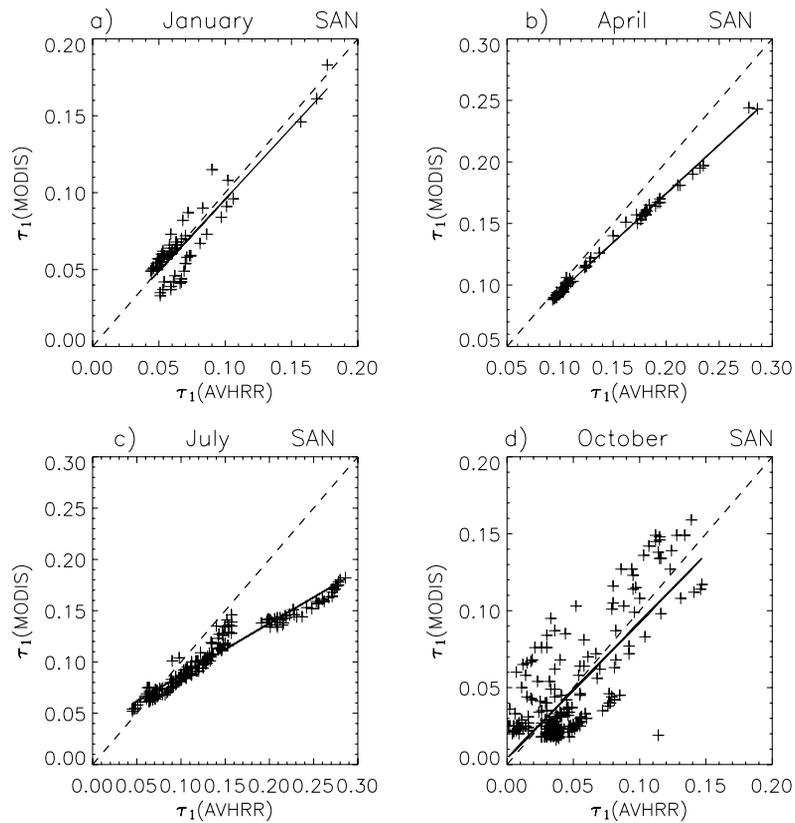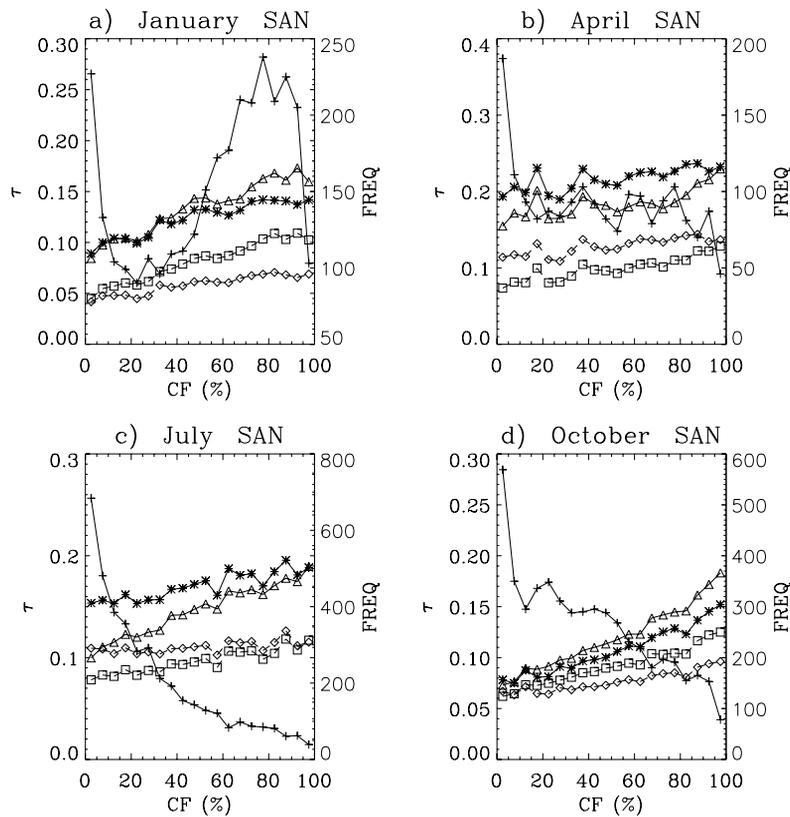

Figure 10. Mean values of τ_1 and τ_2 from MODIS (triangles and squares, respectively) and AVHRR (asterisks and diamonds, respectively) methods for SAN as functions of Cloud Fraction during 2001. Plus signs are number (frequency) of footprints used for averaging in each CF bin.
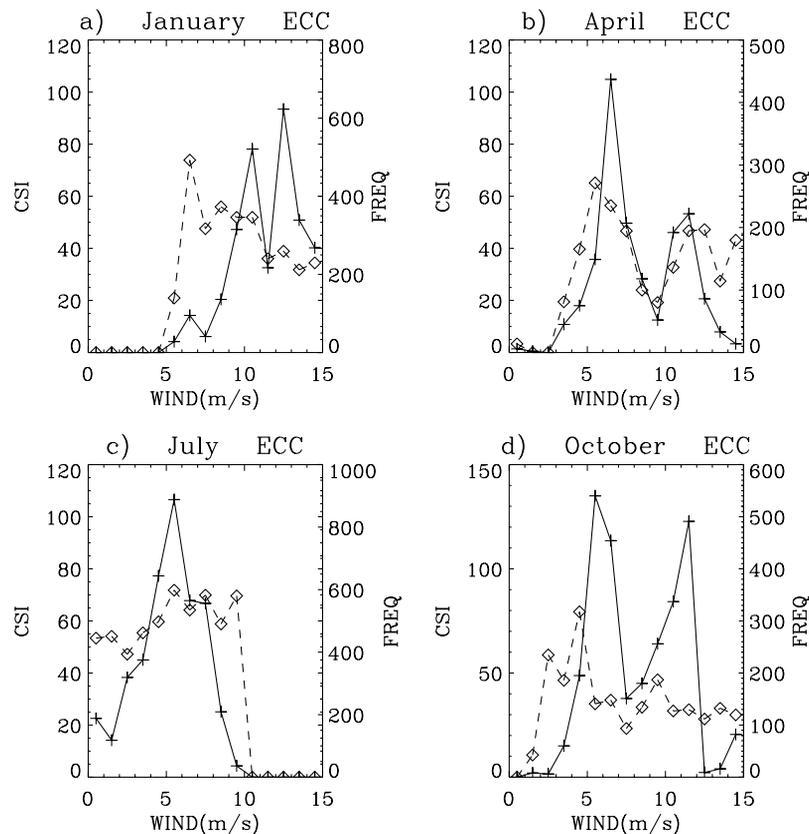
Figure 11. SSF CSI (diamonds) averaged for ECC site as functions of surface wind speed during 2001. Plus signs are number (frequency) of footprints used for averaging in each bin.

when continental aerosols are present. Indeed, like the example shown in Figure 8, the τ_1(MODIS) agrees very well with the τ_1(AVHRR) during January but is systematically lower than τ_1(AVHRR) in April. The differences during spring and summer then are likely to be due mostly to the differences in the aerosol models. There are no SSF data for the clearest and smoothest category in July and October because of persistent high wind speeds and rough surfaces.

3.2. Group Two Analysis

[22] In the regional comparison for SAN in Figure 1, AOT(MODIS) exceeds AOT(AVHRR) in January and October but not during April and July. A similar result was found for the clearest and smoothest conditions during April and July suggesting that the model differences are again responsible for the spring-summer discrepancies. The differences between the two retrievals of τ_1 plotted in Figure 9 for the clearest and smoothest conditions confirm this conclusion. During April and July, the two τ_1s are in good agreement as they approach zero, but they diverge for larger values, which fits the classic result for using incorrect assumptions in the aerosol model [*Zhao et al.*, 2002, 2003]. It is also known that marine aerosols prevail over SAN because of mostly onshore flow during fall and winter, while air pollution over the western coast of the United States may advect over the site in late spring and summer because of a mixture of onshore and offshore winds. The AVHRR-type retrieval agrees well with the

MODIS retrieval for marine aerosols in January and October as expected. However, the two retrievals disagree for the more polluted conditions during April and, especially, July. The good agreement at the low end of the range during the warmer months indicates that marine aerosols probably dominate when AOT is small and the pollution aerosols prevail when AOT is large.

[23] Interestingly, for the SSF footprints that satisfy the retrieval criteria, more of them occur in weak clear conditions (larger CF) in January and October while more SSF footprints occur in strong clear and clear conditions during April and July (Figure 10). It has been observed in the previous global analysis that, for aerosols in the moist environment around clouds, AOT(MODIS) tends to be larger than AOT(AVHRR). Thus the relatively strong cloud effect in January and October results in AOT(MODIS) exceeding AOT(AVHRR). The relatively weak cloud effect in April and July, however, is not sufficient to offset the relatively large difference in AOT resulting from different aerosol model assumptions used in the two retrievals.

[24] At ECC, the surface wind is very strong in winter and fall, moderate during spring, and small in summer. For example, the mean surface wind speed in January is about 13 m/s. Only a few samples satisfy SWS < 6 m/s in January and SWS < 3 m/s in October and April. Coincidentally, more pixels with high surface wind speed at this site are subject to more cloud influence (smaller CSI) in January and October as observed in Figure 11. Thus the specific feature observed in Figure 1 at this site in January and October
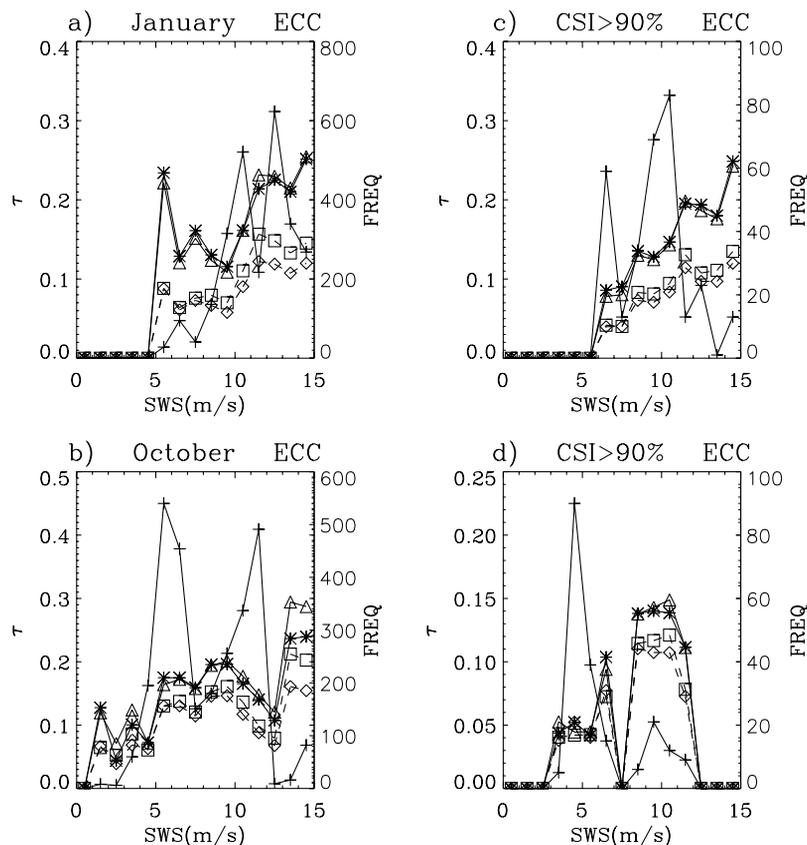
Figure 12. Same as Figure 10 except as functions of surface wind speed (SWS) for (a) January and (b) October original SSF data and (c and d) strong clear condition.

must be associated with effects from both clouds and surface roughness.

[25] In Figure 12, τ_1 and τ_2 averages for the original and case 2 conditions at the ECC site are plotted as functions of SWS for January and October along with the number (frequency) of footprints used for averaging in each SWS interval. Comparing Figure 12a with Figure 12c and Figure 12b with Figure 12d indicates that the cloud effect at SWS > 10 m/s for channel 1 (0.66 μm) causes τ_1(MODIS) to exceed τ_1(AVHRR). However, the surface roughness and cloud effects are comparable causing τ_2(MODIS) to increase relative to τ_2(AVHRR). The surface roughness has more impact at 1.60 μm than at 0.66 μm. The differential effect of surface roughness on AOT for the two channels at high wind speeds was also noticed for the results using similar channels on the Tropical Rainfall Measuring Mission Visible Infrared Scanner (TRMM/VIRS) [*Zhao et al.*, 2003]. The relatively large spectral difference in whitecap reflectance at large wind speeds between the visible and near infrared channels [see *Moore et al.*, 2000] may be responsible for the difference. However, more investigation is necessary before reaching a final conclusion about the differential spectral impact. Such research is beyond the scope of this study.

3.3. Group Three Analysis

[26] SAT in the last group is a typical marine site in the remote South Atlantic Ocean. Figure 13 shows scatterplots of τ_1(MODIS) versus τ_1(AVHRR) for the strong clear case (CSI > 90%) during January, April, July, and October. The

τ_1(AVHRR) values are somewhat higher than their MODIS counterparts during January and October but lower in April and July. These differences are not likely due to the cloud effect since it has been minimized in the strong clear case. Interestingly, similar features are also observed in the scatterplots for the original data (c.f. third column in Figure 2) and the clearest and smoothest case (not shown). These results suggest that the explanations for the positive $\Delta\tau$ in January and October and the negative $\Delta\tau$ in April and July observed at SAT in Figure 1 should be sought from surface disturbance or aerosol model assumptions.

[27] A globally fixed aerosol model with monomodal lognormal size distribution and refractive index of 1.40 + 0.00i was used in the AVHRR retrieval [*Ignatov et al.*, 2004] to represent the global mean condition. However, four fine modes (all with some absorption) and five coarse modes were adopted and combined to form a bimodal size distribution being used in the MODIS retrieval method [*Remer et al.*, 2005]. These model differences can produce differences in the retrieved aerosol optical properties even for a marine aerosol site such as SAT. They are expected to be larger for high τ values than for low τ values and produce the well-demonstrated slope divergence for the linear regression in the scatterplot of AOT from the two retrieval algorithms. Thus the gradual departure of the linear fit from the 1:1 relationship as τ_1 increases in Figures 13a and 13d should be mainly due to aerosol model differences.

[28] On the other hand, the offset for small AOTs in the scatterplot is mainly related to inaccurate surface
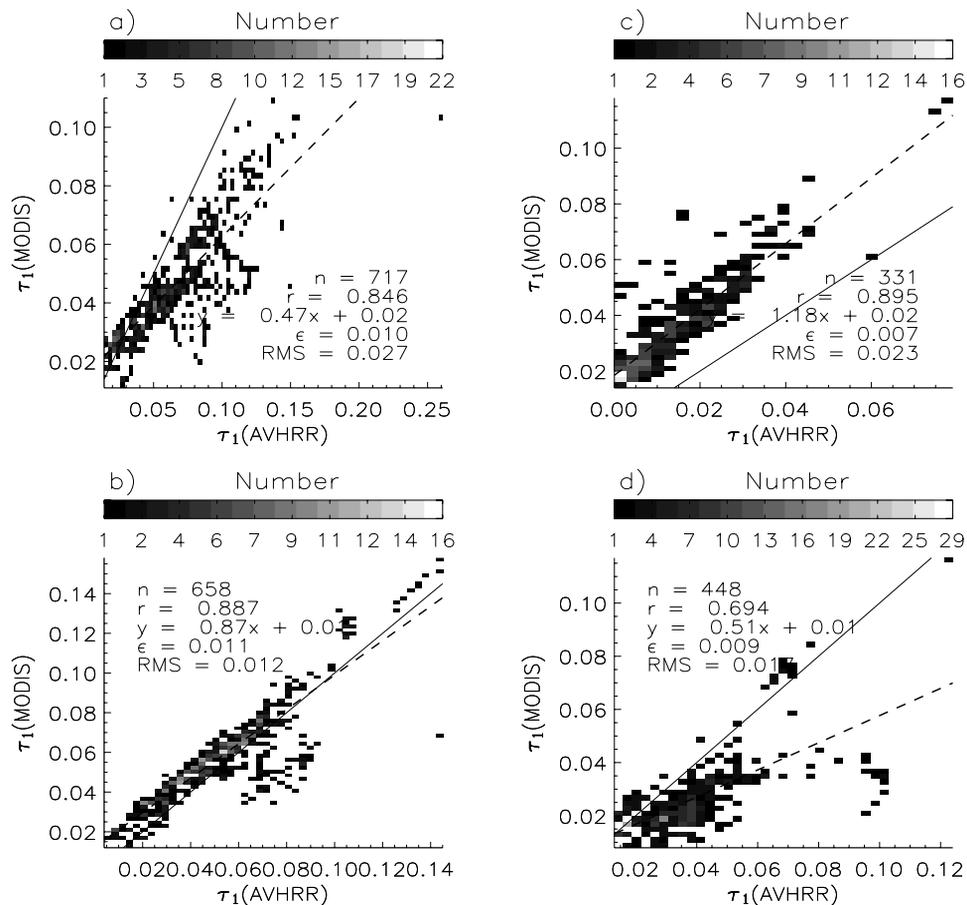
Figure 13. Scatterplots of τ_1(MODIS) versus τ_1(AVHRR) during (a) January, (b) April, (c) July, and (d) October 2001 for CSI > 90% at SAT site. Solid line is 1:1 relationship. Dashed line is linear fit (formula is also shown).

treatment in the algorithm formulations. Thus the offset of the linear fit (dashed line) in Figures 2 and 13, especially for July (Southern Hemisphere winter), should be related to the surface disturbance. To examine this issue, the monthly mean values of size parameter α (or Ångström exponent) at SAT are plotted in Figure 14 according to SWS for both the original data and the strong clear cases. The size parameter, compared to AOT, is more sensitive to errors associated with surface disturbances than to those due to poor aerosol model assumption at low AOT values [*Ignatov and Stowe*, 2000; *Zhao et al.*, 2002].

[29] During January (Figures 14a and 14e), April (Figures 14b and 14f), and October (Figures 14d and 14h), the major α difference occurs at small surface wind speed (SWS < 5 m/s). This is probably due to the use of different surface wind speeds (6 m/s for MODIS; 1 m/s for AVHRR) in the computation of surface reflectance for the two retrievals. In July (Figures 14c and 14g), α is negative for both methods, especially for the AVHRR technique, which yields values outside of a realistic range (0 < α < 3). This abnormality in α during July strongly suggests an effect of a surface disturbance, such as residual whitecap contamination or sun glint effect, on the satellite aerosol retrievals. This indication is also supported by the occurrence of stronger surface wind speeds and a rougher ocean surface in the winter season

of the remote South Atlantic Ocean. However, more study is needed to identify the exact nature of the surface disturbance that is responsible for the distorted α.

[30] Both SIN and SPC are in the 40°S–60°S "roaring forties" band [*Yu et al.*, 2003]. Large marine AOTs are observed in these latitudes, which may be attributable to the large sea salt production [e.g., *Chin et al.*, 2002] a real physical phenomenon, and also to possible retrieval artifacts such as whitecap contamination [*Higurashi and Nakajima*, 1999] and sun glint effect [*Yu et al.*, 2003], all resulting from high winds. These explanations are based on the fact that surface winds are very strong in the "roaring forties" band. For example, at SPC, the average SWS is close to the global mean (6 m/s) in January and larger in April, July, and October (especially in July). Analysis was performed for both the SPC and SIN but only the results for the SPC site are presented below since the results for the two sites are very similar.

[31] As shown in Figure 15 for τ_1, the aerosol retrievals at the SPC site agree well, on average, for CSI > 90% and SWS < 3 m/s in January, April, and October (note that no footprints with SWS < 3 m/s were found in July). This result was expected since the prevailing aerosol type over the "roaring forties" band is sea salt, which is assumed in the AVHRR retrieval and is also included in the dynamical aerosol models of the MODIS method. Figure 16 displays τ_1 and τ_2 averaged for the SPC according to SWS for the
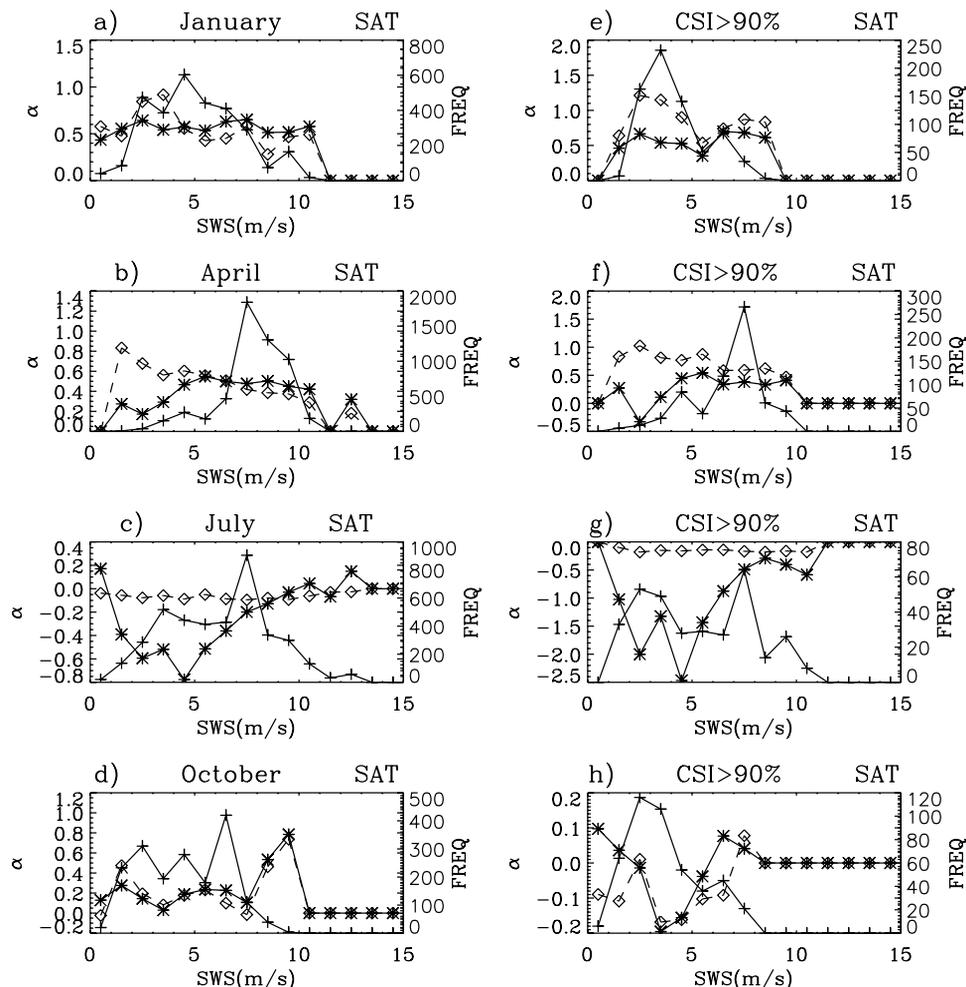
Figure 14. Average α(MODIS), diamonds, and α(AVHRR), asterisks, for SAT site as functions of surface wind speed during 2001 for (a–d) original SSF data and (e–h) for CSI > 90%. Number (frequency) of footprints in each bin is shown as plus signs.

original data (Figures 16a–16d) and for CSI > 90% (Figures 16e–16h) to separate the surface roughness and cloud effects. The variation of AOT with cloud fraction is plotted in Figure 17.

[32] In January (Figures 16a and 16e), AOT increases slightly with wind speed, which is probably attributable to the larger sea salt production at high winds as suggested by *Chin et al.* [2002]. A minor cloud effect on the two aerosol retrievals is also noticed at moderate SWS. The majority of the footprints occur in strong clear conditions (Figure 17a) when AOT(AVHRR) is slightly greater than AOT(MODIS). When the cloud effect becomes sufficiently strong, at CF > 70%, the relationship changes and AOT(MODIS) is 20% greater than AOT(AVHRR). In April and October, the majority of the footprints are associated with a broad range of surface wind speeds (5–11 m/s), even for strong clear conditions. The number of footprints satisfying the retrieval criteria is reduced significantly for both retrievals in April and October compared to January. The MODIS AOTs are systematically higher than their AVHRR counterparts; τ_2(MODIS) value is even larger than the τ_1(AVHRR), regardless of cloud coverage (Figure 17). Even fewer footprints satisfy the retrieval criteria during July. For this

limited number of footprints, τ_2(MODIS) again exceeds τ_1(AVHRR) and is nearly equal to τ_1(MODIS).

[33] The occurrence of fewer footprints suitable for aerosol retrieval due to strong surface wind speeds in April, July, and October and the abnormal characteristic of AOT ($\tau_2 \geq \tau_1$) in the two SSF aerosol products in July suggest that the residual sun glint effect or whitecaps contamination affect the two retrievals (especially in July), which is consistent with the suggestion of a surface disturbance in the "roaring forties" band by *Yu et al.* [2003] and *Higurashi and Nakajima* [1999]. However, more research is needed to determine if it is whitecap contamination, the sun glint effect, or both causing the disturbance. Since α is more sensitive to a surface disturbance than the AOT, the scatterplots of α(MODIS) versus α(AVHRR) in Figure 18 should provide more insight about the anomalous behavior of the spectral AOTs for this site. More α(AVHRR) than α(MODIS) values fall in an unrealistic range, especially during July. These analyses indicate that the impact of the surface disturbances on the AVHRR retrieval is probably more severe than on the MODIS retrieval, although further improvement of the surface model for a rough ocean surface is needed for the both
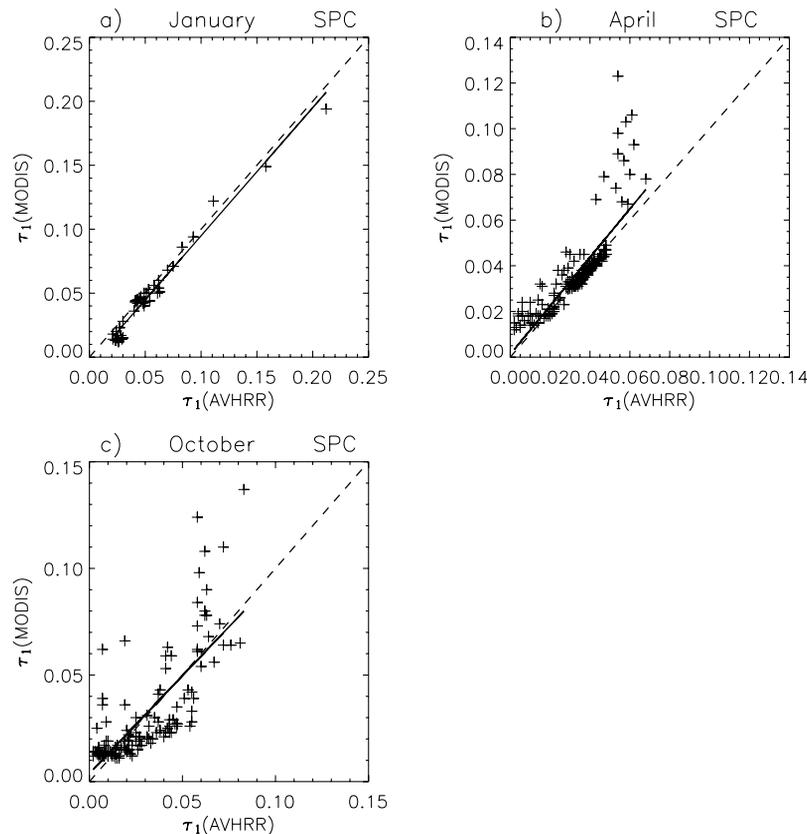
Figure 15. Same as Figure 7 except for SPC site.

retrievals. The cloud effect is minor compared to the surface disturbance in the "roaring forties" band since the pixels contained in the footprints with the aerosol retrievals are dominated mainly by the clear sky condition (Figure 17).

3.4. Discussion

[34] Obtaining long-term global aerosol data useful for studying long-term aerosol effects on climate is one of the most urgent issues being considered by the aerosol research community. As pointed out by *Zhao et al.* [2005], a feasible approach is to build a connection and establish consistency between the historical AVHRR and more advanced MODIS aerosol retrievals so that the two observations along with those from the future satellite sensors (such as the VIIRS on the NPOESS satellite) can be combined eventually to form long-term global aerosol data useful for long-term aerosol climate studies. Since the MODIS and AVHRR retrieval algorithms differ in many aspects, it is logical to expect disagreements in their retrieved aerosol properties. Reconciling these differences is a key to obtaining the desired long-term aerosol record. However, how can this be accomplished?

[35] First, we understand that the issue of cloud effects discussed in this study cannot be easily resolved in the near future but they apparently impact aerosol retrievals on both regional and global scales. Thus we believe that the cloud effect should be avoided as much as possible in the formation of the long-term aerosol data from various satellite sensors before the issue is clearly resolved. In other words, as the first effort, only the clearest pixels or grids should be selected when combining data from different

satellite sensors. To do this, all appropriate satellite aerosol products should be reprocessed to include a cloud-screening quality flag at the pixel or grid level. Only the product grids that pass all cloud screening tests of a cloud mask scheme should be selected and any product grids satisfying a relaxed cloud screening should not be included but can be flagged for future reprocessing.

[36] Second, after removing the retrieval uncertainties associated with cloud effects, the current results indicate that the AVHRR and MODIS retrieval methods over the oceans yield similar AOT values in a global average. As a result, large errors introduced in the estimation of global oceanic mean aerosol climate effect from AVHRR aerosol data are not be expected big. However, large AOT differences occur in various regions when aerosols are advected from land masses (including smoke, dust, and industrial pollution) and when winds roughen ocean surfaces (such as the 40°S–60°S "roaring forties" band). Thus a great caution is necessary when applying the historical AVHRR aerosol data for the study of aerosol climate effect in a specific region, especially over areas where anthropogenic aerosols and/or rough ocean surfaces are common. Detailed analyses similar to those used here should be performed for the region before applying the satellite aerosol data to long-term climate studies. Such analyses should provide baseline offsets that could be used to adjust the regional data.

[37] Last, an important issue for long-term aerosol climate study that was not considered here is the need to apply a consistent calibration to the historical and current AVHRR, MODIS, and future satellite sensors. Calibration inconsistencies need to be eliminated for the same sensor
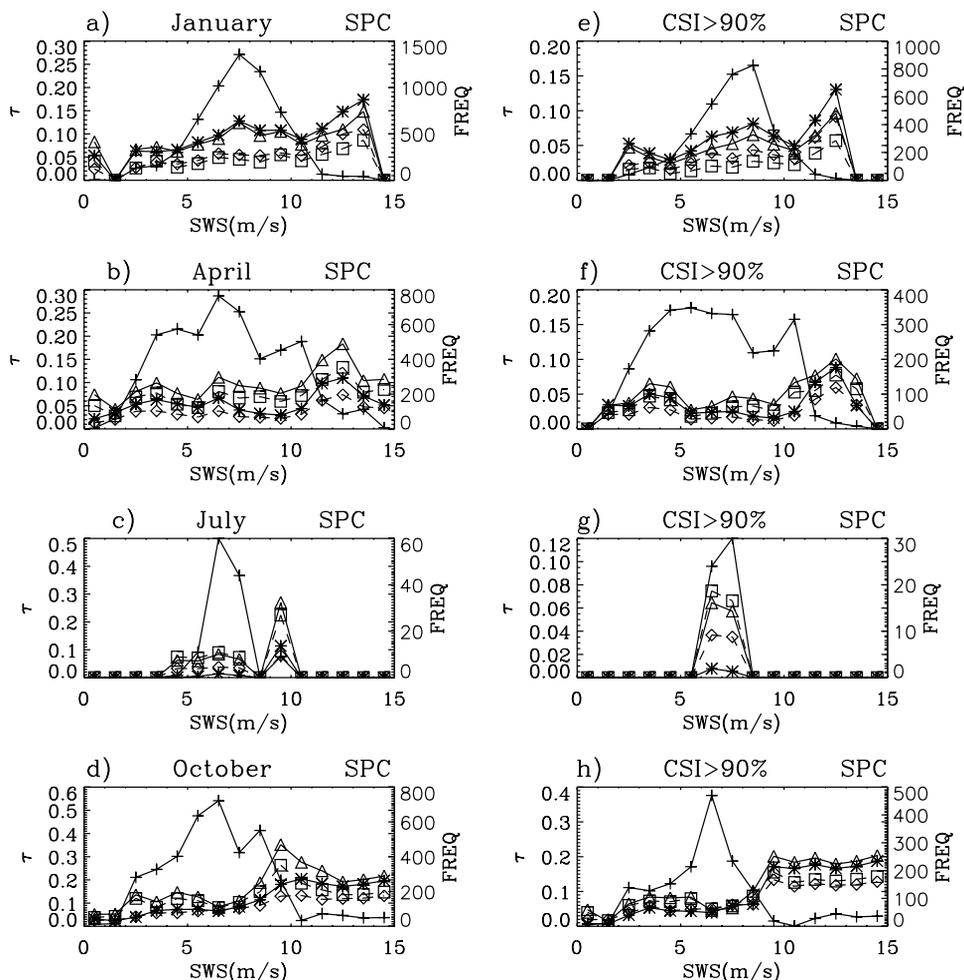
Figure 16. (a–h) Same as Figure 12 except for 4 months at SPC site.

flying on different satellite platforms, such as the AVHRR on NOAA 7, 9, 11, 14, 15, 16 and 17 and the MODIS on Terra and Aqua. Thus intersatellite calibrations [e.g., *Minnis et al.*, 2002] should be developed before combining the AVHRR and MODIS measurements for aerosol climate studies. To support long-term climate studies, the AVHRR Pathfinder Atmosphere (PATMOS) climate data set is being reprocessed at the Office of Research and Application (ORA) of NOAA/NESDIS to include a new calibration based on the Simultaneous Nadir Overpass method developed specifically for intersatellite calibration of radiometers [*Cao et al.*, 2004; *Heidinger et al.*, 2002]. Specifically, more accurate MODIS radiances (with ±2% uncertainty determined from onboard calibration) are used to cross-calibrate the AVHRR radiances (with ±5% uncertainty determined from vicarious calibration) of the NOAA polar-orbiting satellites that their span of operational time overlaps with that of MODIS. The newly calibrated AVHRR radiances are applied backward one platform each time until the last (or the earliest) platform is completed. As a result, the MODIS calibration is effectively transferred to the AVHRR with uncertainties close to that of MODIS. Most importantly, a consistent calibration (critical for a study of long-term aerosol climate effect) is obtained for the new PATMOS data (named PATMOS-X). The two
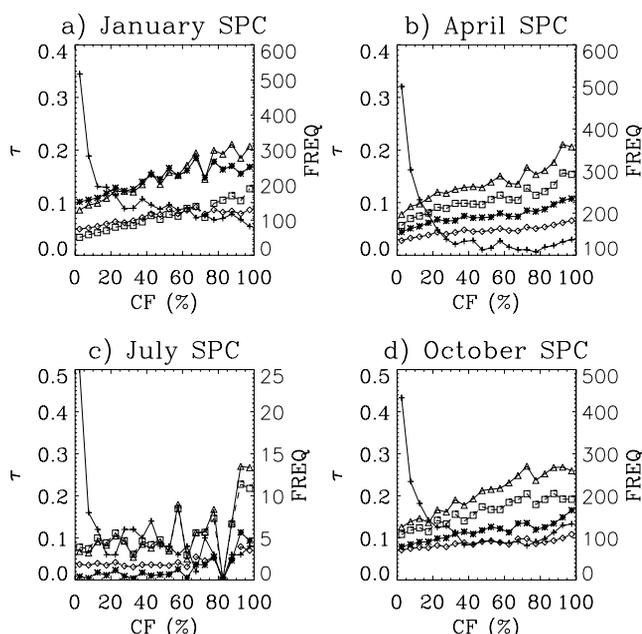

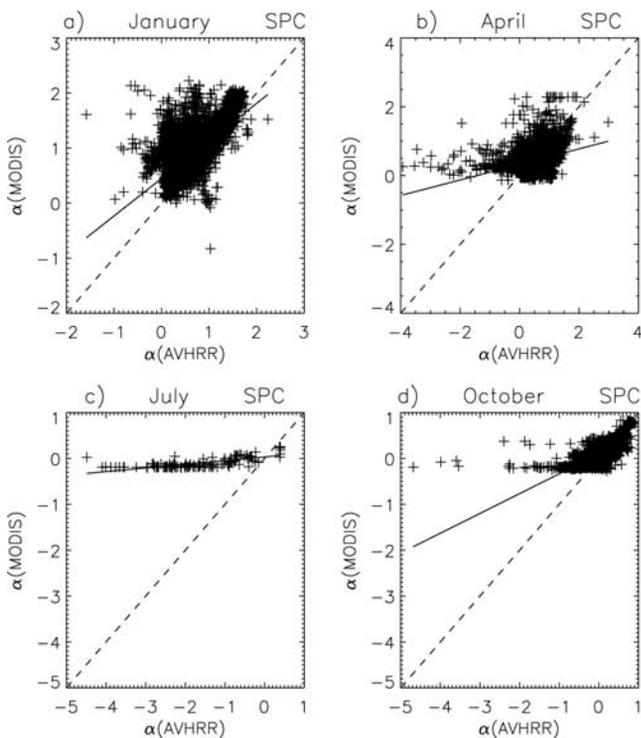**Figure 17.** (a–d) Same as Figure 10 except for SPC site.

Figure 18. Same as Figure 7 except for size parameter at SPC site.

versions of PATMOS data with different calibrations provide a good opportunity to study the calibration effect on the AVHRR aerosol retrievals and to evaluate quantitatively the importance of a consistent calibration for the study of long-term aerosol climate effect from space. We are preparing these studies and the results will be presented in future publications.

4. Summary and Conclusions

[38] The MODIS and NOAA/NESDIS AVHRR-type aerosol retrievals were compared on a regional scale. This comparison is a necessary initial step toward establishing connection and consistency between the advanced multichannel MODIS and the simple independent two-channel AVHRR aerosol retrieval methods. As in the global evaluation presented in part 1 of this work [Zhao et al., 2005], the two aerosol products derived respectively from the MODIS and AVHRR retrievals in the Terra/CERES-MODIS SSF data were used in the comparison and analyses. Scatterplot and probability distribution analysis techniques along with several statistical parameters were used for a detailed comparison. The effects of aerosol model assumptions and cloud and surface roughness on the two retrievals were analyzed through the careful classification of clear-sky and surface conditions by taking advantage of the multiple parameters included in the SSF data.

[39] Nineteen locations were selected for the regional comparison and analyses. For most of the regions, the annual mean difference of the aerosol optical thickness from the MODIS and AVHRR retrievals is less than 0.03 and 0.02, respectively, at 0.66 μm and 1.60 μm. Since a change of 0.01 in the global mean aerosol optical thickness

can yield a 0.25 W/m^2 flux change [Mishchenko et al., 2004], a difference of $0.02-0.03$ in the global mean aerosol optical thickness is not trivial. In general, the MODIS aerosol optical thickness is somewhat less than that from the AVHRR retrieval for the selected locations. However, the situation can be reversed in certain regions that are primarily under the influence of cloud or greater than average surface wind speeds. In agreement with the results of the global comparison [Zhao et al., 2005], the regional comparison further confirm that aerosol model assumptions, cloud effects, and surface roughness are the three major contributors to the major differences between the two retrieval techniques. However, significantly large differences between the two retrievals were only observed in regions with strong seasonal variations in the prevailing aerosol type, or under the influence of high surface wind speed and in the scenarios with relatively high coverage of clouds. The correlation analyses performed here are helpful for identifying possible causes of the regional difference in the two SSF aerosol products. The ensemble validation of the two SSF aerosol products against the ground-based AERONET observations indicates that both satellite aerosol products are subject to some residual subpixel cloud contamination. On average, it was found that the two methods tend to overestimate 0.66-μm aerosol optical thickness (AOT) compared to AERONET surface observations in the original SSF data. If the most cloud-free data are used, the mean satellite retrievals agree to within ±10% of the AERONET data. The MODIS near-infrared (1.60 μm) AOTs are in better agreement with the surface data than the AVHRR retrievals. For pixels with minimal cloud contamination, the size parameter α from the multichannel MODIS retrieval is in better agreement with the AERONET results than that derived from the two-channel AVHRR algorithm.

[40] Although, in the global correlation analysis of surface roughness effects, it was found that wind driven aerosols play a dominant role compared to the retrieval errors associated with the surface disturbance for most of the ocean surfaces. One exception was identified using the current regional correlation analysis. In the "roaring forties" band of the Southern Hemisphere (especially in the winter season) it was concluded that sun glint effects and whitecap contamination appear to be more important than wind-driven aerosols in producing errors. Even though, the computation of surface reflectance in the MODIS and AVHRR retrieval algorithms are comparable in a global mean sense, the difference becomes noticeable over windy areas, where the surface treatment used in the MODIS retrieval performs somewhat better than that used in the AVHRR retrieval. However, further improvement of both surface treatments is needed to accurately interpret marine aerosols in rough ocean conditions. We also conclude the aerosol model assumption becomes important for regional retrievals, especially for areas with strong seasonal variations in the prevailing aerosol type. The dynamic aerosol models used in the MODIS retrievals are better in simultaneously capturing the regional variations of aerosol optical properties and their global mean values.

References

Cao, C., M. Weinreb, and H. Xu (2004), Predicting simultaneous nadir overpasses among polar-orbiting meteorological satellites for the inter-satellite calibration of radiometers, *J. Atmos. Oceanic Technol.*, *21*, 537–542.

Chin, M., P. Ginoux, S. Kinne, O. Torres, B. Holben, B. N. Duncan, R. V. Martin, J. A. Logan, A. Higurashi, and T. Nakajima (2002), Aerosol distributions and radiative properties simulated in the GOCART model and comparisons with observations, *J. Atmos. Sci.*, *59*, 461–483.

Dubovik, O., B. N. Holben, T. E. Eck, A. Smirnov, Y. J. Kaufman, M. D. King, D. Tanre, and I. Slutsker (2002), Variability of absorption and optical properties of key aerosol types observed in worldwide locations, *J. Atmos. Sci.*, *59*, 590–608.

Heidinger, A. K., C. Cao, and J. Sullivan (2002), Using Moderate Resolution Imaging Spectrometer (MODIS) to calibrate Advanced Very High Resolution Radiometer (AVHRR) reflectance channels, *J. Geophys. Res.*, *107*(D23), 4702, doi:10.1029/2001JD002035.

Higurashi, A., and T. Nakajima (1999), Development of a two channel aerosol retrieval algorithm on global scale using NOAA/AVHRR, *J. Atmos. Sci.*, *56*, 924–941.

Holben, B. N., et al. (1998), AERONET—A federated instrument network and data archive for aerosol characterization, *Remote Sens. Environ.*, *66*, 1–16.

Holben, B. N., et al. (2001), An emerging ground-based aerosol climatology: Aerosol optical depth from AERONET, *J. Geophys. Res.*, *106*, 12,067–12,097.

Ignatov, A., and L. L. Stowe (2000), Physical basis, premises, and self-consistency checks of aerosol retrievals from TRMM/VIRS, *J. Appl. Meteorol.*, *39*, 2259–2277.

Ignatov, A., J. Sapper, S. Cox, I. Laszlo, N. R. Nalli, and K. B. Kidwell (2004), Operational aerosol observations (AEROBS) from AVHRR/3 on board NOAA-KLM satellites, *J. Atmos. Oceanic Technol.*, *21*, 3–26.

Intergovernmental Panel on Climate Change (2001), *Climate Change 2001: The Scientific Basis*, 870 pp., Cambridge Univ. Press, New York.

Kaufman, Y. J., D. Tanré, and O. Boucher (2002), A satellite view of aerosols in the climate system, *Nature*, *419*, 215–223.

King, M. D., Y. J. Kaufman, D. Tanré, and T. Nakajima (1999), Remote sensing of tropospheric aerosols: Past, present, and future, *Bull. Am. Meteorol. Soc.*, *80*, 2229–2259.

Minnis, P., L. Nguyen, D. R. Doelling, D. F. Young, W. F. Miller, and D. P. Kratz (2002), Rapid calibration of operational and research meteorological satellite imagers, part I: Evaluation of research satellite visible channels as references, *J. Atmos. Oceanic Technol.*, *19*, 1233–1249.

Mischenko, I. M., I. V. Geogdzhayev, B. Cairns, W. B. Rossow, and A. Lacis (1999), Aerosol retrievals over the oceans by use of channels 1 and 2 AVHRR data: Sensitivity analysis and preliminary results, *Appl. Opt.*, *38*, 7325–7341.

Mischenko, I. M., B. Cairns, J. E. Hansen, L. D. Travis, R. Burg, Y. J. Kaufman, J. V. Martins, and E. P. Shettle (2004), Monitoring of aerosol forcing of climate from space: Analysis of measurement requirements, *J. Quant. Spectrosc. Radiat. Transfer*, *88*, 149–161.

Moore, K. D., K. J. Voss, and H. R. Gordon (2000), Spectral reflectance of whitecaps: Their contribution to water-leaving radiance, *J. Geophys. Res.*, *105*, 6493–6499.

Remer, L. A., et al. (2005), The MODIS aerosol algorithm, products and validation, *J. Atmos. Sci.*, *62*, 947–973.

Smirnov, A., B. N. Holben, T. F. Eck, O. Dubovik, and I. Slutsker (2000), Cloud screening and quality control algorithms for the AERONET data base, *Remote Sens. Environ.*, *73*, 337–349.

Tanré, D., M. Herman, and Y. J. Kaufman (1996), Information on the aerosol size distribution contained in the solar reflected spectral radiances, *J. Geophys. Res.*, *101*, 19,043–19,060.

Yu, H., R. E. Dickinson, M. Chin, Y. J. Kaufman, B. N. Holben, I. V. Geogdzhayev, and M. I. Mishchenko (2003), Annual cycle of global distributions of aerosol optical depth from integration of MODIS retrievals and GOCART model simulations, *J. Geophys. Res.*, *108*(D3), 4128, doi:10.1029/2002JD002717.

Zhao, X., L. Stowe, A. Smirnov, D. Crosby, J. Sapper, and C. R. McClain (2002), Development of a global validation package for satellite oceanic aerosol optical thickness retrieval based on AERONET observations and its application to NOAA/NESDIS operational aerosol retrievals, *J. Atmos. Sci.*, *59*, 294–312.

Zhao, X., I. Laszlo, B. N. Holben, C. Pietras, and K. J. Voss (2003), Validation of two-channel VIRS retrievals of aerosol optical thickness over ocean and quantitative evaluation of the impact from potential sub-pixel cloud contamination and surface wind effect, *J. Geophys. Res.*, *108*(D3), 4106, doi:10.1029/2002JD002346.

Zhao, X., O. Dubovik, A. Smirnov, B. N. Holben, J. Sapper, C. Pietras, K. J. Voss, and R. Frouin (2004), Regional evaluation of an advanced very high resolution radiometer (AVHRR) two-channel aerosol retrieval algorithm, *J. Geophys. Res.*, *109*, D02204, doi:10.1029/2003JD003817.

Zhao, X., I. Laszlo, P. Minnis, and L. Remer (2005), Comparison and analysis of two aerosol retrievals over the ocean in the Terra/Clouds and the Earth's Radiant Energy System–Moderate Resolution Imaging Spectroradiometer single scanner footprint data: 1. Global evaluation, *J. Geophys. Res.*, *110*, D21208, doi:10.1029/2005JD005851.

————————————

I. Laszlo and T. X.-P. Zhao, Office of Research and Application, NOAA National Environmental Satellite, Data, and Information Service, 5200 Auth Road, Camp Springs, MD 20746, USA. (xuepeng.zhao@noaa.gov)

P. Minnis, Atmospheric Sciences Division, NASA Langley Research Center, Hampton, VA 23681, USA.

L. Remer, Laboratory for Atmospheres, NASA Goddard Space Flight Center, Greenbelt, MD 20771, USA.